Noncovalent Immobilization of a Nickel Cyclam Catalyst on Carbon Electrodes for CO_2 Reduction Using Aqueous Electrolyte

Francesca Greenwell, Gaia Neri, Verity Piercy and Alexander J. Cowan*

Supporting information

1. Synthesis

Synthesis of 4-(pyren-1-yl)butanal (**1**): To a solution of 1-pyrenebutanol (1.2 g, 4.3 mmol) in dry DCM (15 ml) under an inert atmosphere, a suspension of pyridinium dichromate (2.5 mg, 6.65 mmol) in dry DCM (15 ml) was added rapidly. The resulting suspension was stirred under argon overnight. The suspension is then diluted with 600 ml of diethyl ether and washed with water first then brine twice. The organic phase was dried over $MgSO_4$, then filtered and the solvent was evaporated. The resulting orange oil was purified using a silica plug eluted with chloroform. Yellow oil, obtained: 900 mg, yield : 75%. ^{1}H NMR (400 MHz, $CDCl_3$): δ 9.75 (s, 1H), 8.25 (d, J = 9.3 Hz, 1H), 8.18 (dd, J = 7.6, 2.0 Hz, 2H), 8.10 (dd, J = 8.5, 4.4 Hz, 2H), 8.03 (s, 2H), 8.02 – 7.99 (m, 1H), 7.80 (d, J = 7.8 Hz, 1H), 3.35 – 3.27 (m, 2H), 2.49 (td, J = 7.2, 1.6 Hz, 2H), 2.15 (p, J = 7.3 Hz, 2H). ^{13}C NMR (101 MHz, $CDCl_3$): δ 200.99, 130.25, 129.71, 128.84, 127.53, 126.32, 126.28, 126.07, 125.60, 124.72, 123.92, 123.82, 123.81, 123.67, 123.65, 122.03, 42.20, 31.33, 22.71.

Synthesis of tri-tert-butyl-11-(4-(pyren-1-yl)butyl)-1,4,8,11-tetraazacyclotetradecane-1,4,8-tricarboxylate (**2**): 976 mg of Boc_3cyclam[1,2] (1.95 mmol) and 800 mg of 1 (2.9 mmol) were added to a round bottom flask containing 4 Å activated molecular sieves under argon and dissolved in dry DCE (20 ml). The solution is stirred for 2 hours under argon at room temperature. Sodium triacetoxyborohydride (827 mg, 3.9 mmol) was added under an Ar blanket and the solution is stirred for 24 hours. The crude solution was washed with three aliquots of 2 M $NaHCO_3$ then the organic fraction was dried over $MgSO_4$, filtered and the solvent was evaporated to yield a yellow oil. The product was isolated by flash column chromatography, eluting first with DCM then with DCM:EtOAc 50:50. Yellow foam, obtained: 1.16 g, yield: 83%. ^{1}H NMR (400 MHz, $CDCl_3$): δ 8.25 (d, J = 9.3 Hz, 1H), 8.15

(ddd, J = 7.9, 3.8, 1.3 Hz, 2H), 8.10 (dd, J = 8.5, 3.2 Hz, 2H), 8.01 (d, J = 2.2 Hz, 2H), 7.98 (d, J = 7.6 Hz, 1H), 7.84 (d, J = 7.8 Hz, 1H), 3.33 (t, J = 7.8 Hz, 7H), 3.26 (s, 7H), 2.55 (s, 2H), 2.41 (t, J = 7.6 Hz, 4H), 1.81 (q, J = 7.6 Hz, 4H), 1.72 (p, J = 7.3 Hz, 2H), 1.61 (s, 4H), 1.45 (d, J = 4.5 Hz, 27H). ^{13}C NMR (101 MHz, $CDCl_3$): δ, 155.65, 136.76, 131.40, 130.88, 129.76, 128.54, 127.50, 127.22, 127.17, 126.54, 125.79, 125.06, 125.00, 124.83, 124.79, 124.65, 123.37, 79.47, 79.30, 55.38, 53.47, 51.46, 46.87, 45.70, 33.49, 29.80, 28.53, 28.48, 26.75.

Synthesis of 1-(4-(pyren-1-yl)butyl)-1,4,8,11-tetraazacyclotetradecane (CycPy **3**): 1.16 g of 2 (1.53 mmol) was dissolved in 15 ml of DCM, then 7.5 ml of TFA are added dropwise at room temperature. The solution is stirred at room temperature until no change is detected in the TLC (DCM:EtOAC 50:50), ca. 6 hours. The solvent is rotary evaporated (MeOH is continually added to aid with complete TFA removal). The crude is purified by passing through an Amberlite IRN-78 twice, eluting with MeOH. Yellow oil, obtained: 620 mg, yield 83%. ^{1}H NMR (400 MHz, $CDCl_3$): δ 8.24 (d, *J* = 9.3 Hz, 1H), 8.13 – 8.02 (m, 4H), 7.98 – 7.89 (m, 3H), 3.30 (t, *J* = 7.7 Hz, 2H), 2.69 – 2.65 (m, 2H), 2.53 – 2.46 (m, 4H), 2.46 – 2.41 (m, 2H), 2.38 (t, *J* = 5.7 Hz, 4H), 2.30 (q, *J* = 6.1, 5.7 Hz, 4H), 2.16 (d, *J* = 5.3 Hz, 2H), 1.64 – 1.53 (m, 2H), 1.49 (t, *J* = 6.2 Hz, 2H), 1.80 (p, *J* = 7.7 Hz, 2H), 1.65 (d, *J* = 7.1 Hz, 2H). ^{13}C NMR (101 MHz, $CDCl_3$): δ 137.19, 131.40, 130.87, 129.67, 128.55, 127.45, 127.31, 127.22, 126.50, 125.76, 124.97, 124.79, 124.77, 124.59, 123.55, 54.69, 54.37, 52.73, 51.32, 49.87, 49.34, 48.57, 47.75, 47.67, 33.50, 30.07, 28.67, 26.49, 26.21. MS (ESI+): m/z calcd. for $C_{30}H_{40}N_4$: 456, found: 457 [M+H$^+$]. CHN microanalysis: anal. calcd. for $C_{30}H_{40}N_4$: C, 78.90, H, 8.83, N, 12.27; found: C, 74.5, H, 9.28, N, 13.54 ($C_{30}H_{40}N_4$*0.6 NH_4OH*H_2O)

2. UV/Vis spectroscopy

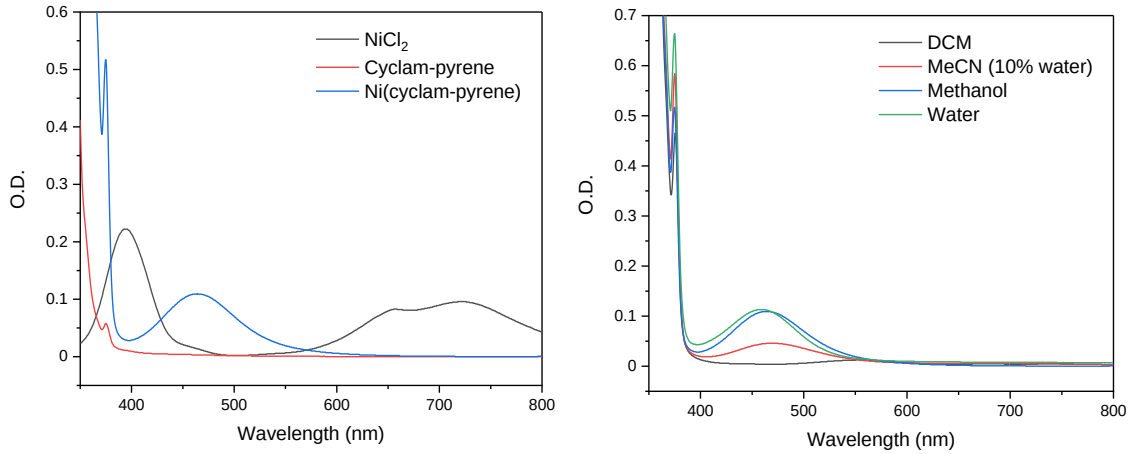

Figure S1 UV/Vis spectrum of CycPy, [Ni(CycPy)].Cl_2 and $NiCl_2$ in water (left) and various solvents (right), 1 mM, pathlength 10 mm

The UV/Vis spectrum of $[Ni(CycPy)]^{2+}$ shows a peak at 463 nm which is assigned to the complex in a square planar form in water.[3]

3. Supporting electrochemical data (solution)

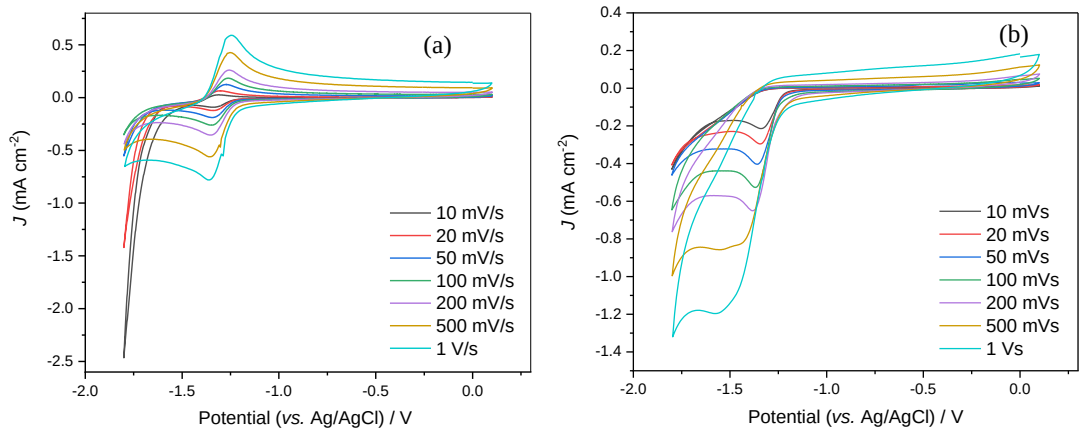

Figure S2 CVs of 1mM $[Ni(CycPy)]^{2+}$ in 0.1M TBA PF_6 CH_3CN with 10% water using a GCE under N_2 (a) and CO_2 (b).

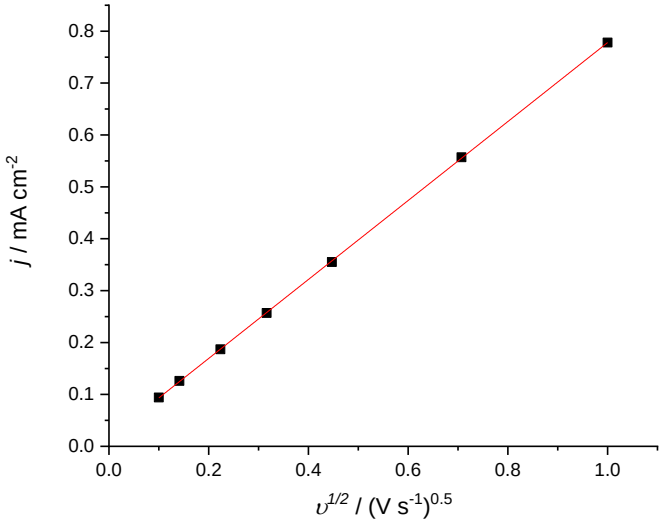

Figure S3 Scan rate dependence of the peak current density of the $Ni^{II/I}$ reduction of 1mM $[Ni(CycPy)]^{2+}$ in 0.1M TBA PF_6 CH_3CN with 10% water using a GCE under N_2.

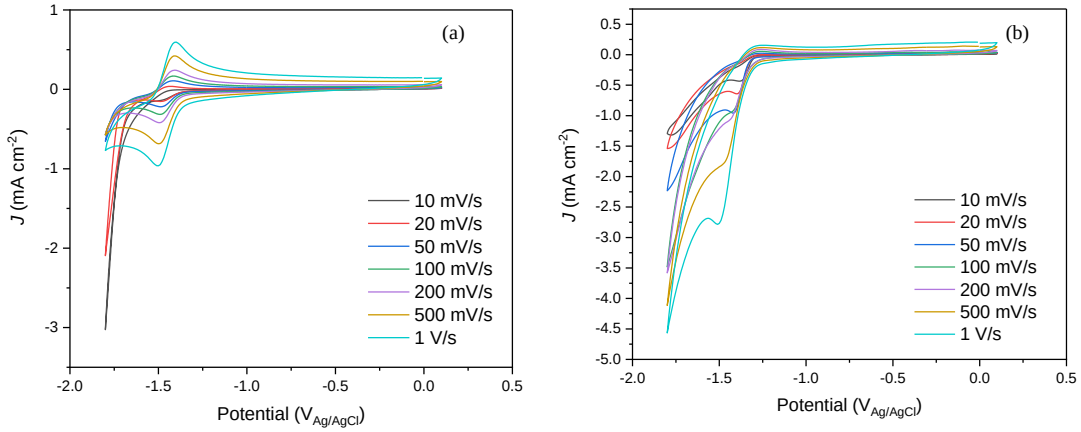

Figure S4 CVs of 1mM $[Ni(Cyc)]^{2+}$ in 0.1M TBA PF_6 CH_3CN with 10% water using a GCE under N_2 (a) and CO_2 (b).

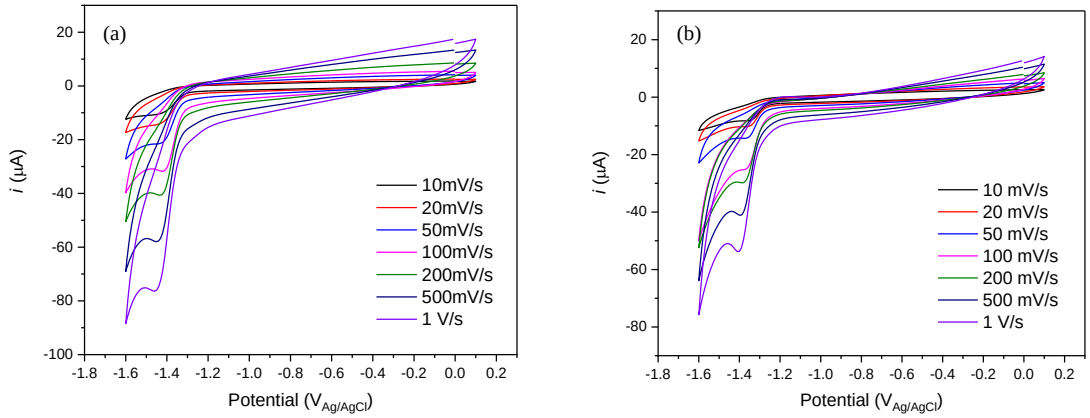

Figure S5 CVs of 1mM $[Ni(CycPy)]^{2+}$ in 0.5M 0.5M $KHCO_3$ under N_2 (a) and CO_2 (b).

Experiments in aqueous solvent were restricted to ≥ -1.6 V. At potentials negative of this the electrochemical features of the $[Ni(CycPy)]^{2+}$ catalyst became diminished and could only be recovered following polishing of the glassy carbon electrode, indicating electrode fouling. In the mixed solvent (CH_3CN/Water (10%)) CV's were recorded to -1.8V with no sign of catalyst degradation.

4. Bulk electrolysis data (non GDE)

Table S1. Bulk electrolysis data

Catalyst	Electrolyte	$V_{Ag/AgCl}$	Time (mins)	J_{avg} (mA cm^{-2})	CO, F.E. (%)	H_2, F.E. (%)	Total FE (%)
0.2 mM $[Ni(CycPy]^{2+}$	$KHCO_3$	-1.40	126	0.17	47	45	92
GCE/[Ni(CycPy]	$KHCO_3$	-1.25	126	0.35	0.6	76	77
GCE/[Ni(CycPy]	$KHCO_3$	-1.40	111	0.31	0.8	86	87

5. XPS:

XPS Analysis was performed using a Thermo NEXSA XPS fitted with a monochromated Al kα X-ray source (1486.7 eV), a spherical sector analyser and 3 multichannel resistive plate, 128 channel delay line detectors. All data was recorded at 19.2 W and an X-ray beam size of 200 x 100 µm. Survey scans were recorded at a pass energy of 160 eV, and high-resolution scans recorded at a pass energy of 20 eV. Electronic charge neutralization was achieved using a Dual-beam low-energy electron/ion source (Thermo Scientific FG-03). Ion gun current = 150 µA. Ion gun voltage = 45 V. All sample data was recorded at a pressure below 10^{-8} Torr and a room temperature of 294 K. Data was analysed using CasaXPS v2.3.19PR1.0. Peaks were fit with a Shirley background prior to component analysis. Lineshapes of LA(1.53,243) were used to fit components.

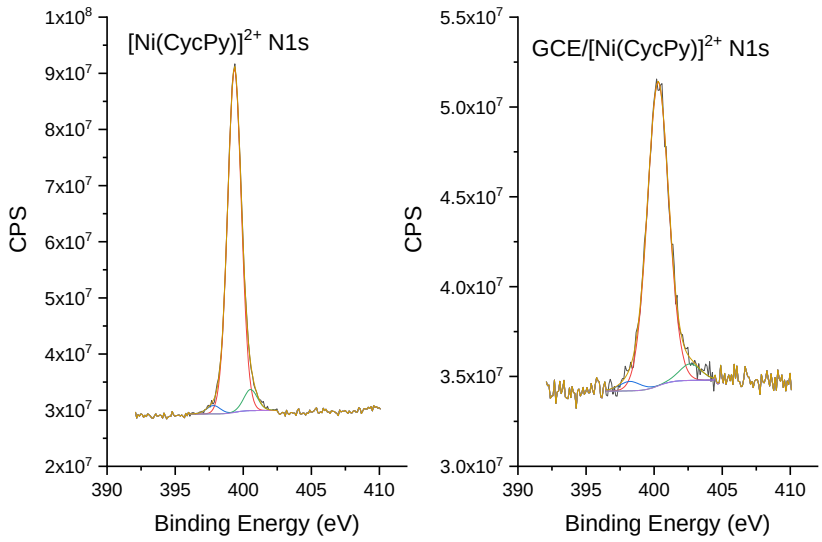

Figure S6 - Experimental and simulated XPS spectra of N1s signal

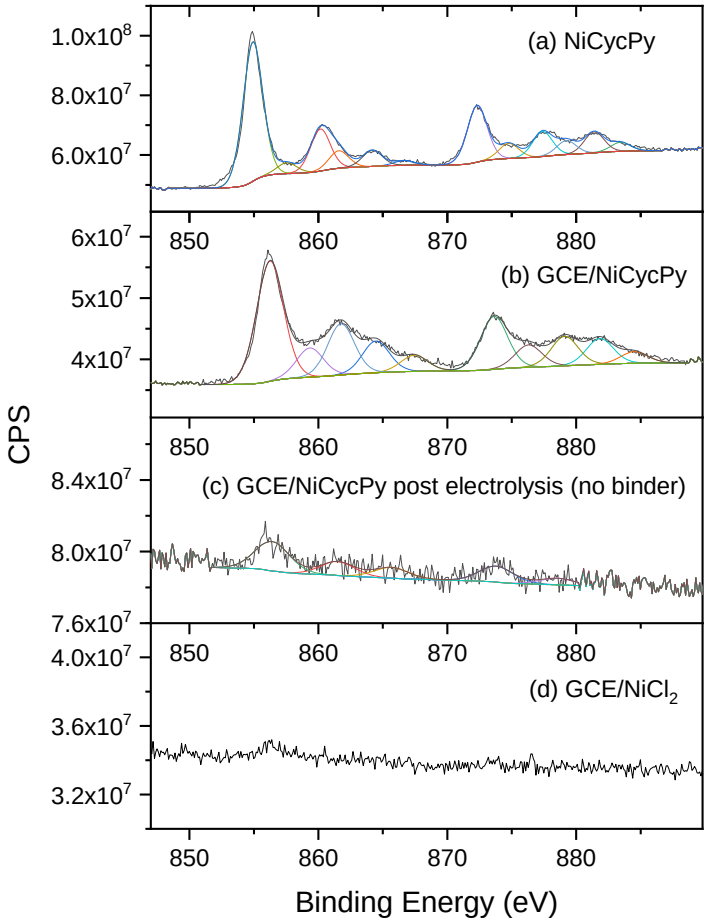

Figure S7 - Experimental and simulated XPS spectra of Ni $2p_{3/2}$ and $2p_{1/2}$ signal

XPS shows the presence of a Ni $2p_{3/2}$ signal at 854.9 eV for the $[Ni(CycPy)]^{2+}$ powder with the Ni $2p_{1/2}$ signal at 872.3 eV . The complex multiplex structure at higher binding energies has been assigned to be only due to Ni^{2+} ions in past reports[4] and the spectrum is in good agreement with previous XPS reports of Ni(II) cyclam complexes.[5–7] Upon immobilisation a strong Ni 2p signal is present (figure S7 b) but is significantly blue shifted (856.2 eV ($2p_{3/2}$) and 873.6 eV ($2p_{1/2}$)). On the basis of reported binding energies for Ni^{III} oxides/hydroxides (typical $2p_{3/2}$ ~856.1 eV)[4] a past study assigned Ni 2p signals at 856.0 eV and 873.8 eV to a Ni^{III}cyclam complex.[8] Conversely a similar pyrene modified Ni cyclam complex reported[9] a Ni^{2+} $2p_{3/2}$ binding energy of 856.0 eV and the trace Ni remaining on a GCE following soaking in $NiCl_2$ has a binding energy of ~856.5 eV. Therefore whilst the XPS data of the GCE/[Ni(CycPy)] electrode provides good evidence of a redistribution of electron density from the Ni centre to the carbon electrode/pyrene group the formal oxidation state of the Ni centre of

GCE/[Ni(CycPy)] during the XPS measurement is not assigned. However, electrochemical data recorded once the electrode is placed in solution suggests that the first reduction that is identified upon initiating a negative sweep from close to the open circuit potential is a $Ni^{II/I}$ reduction (see main text).

Bulk electrolysis experiments on gas diffusion electrodes require the use of Nafion/PTFE mixes to control proton transport pathways and prevent flooding. The high concentration of fluorine containing species means that weak Ni 2p responses are often masked by the F auger peak. Therefore we have instead reported the XPS spectrum of a GCE post electrolysis in $KHCO_3$ electrolyte (-1.4 V for 1 h). This shows a clear loss of Ni from the electrode surface figure S7 (c), but no significant shift in the binding energies when compared to the pre-electrolysis GCE/[Ni(CycPy)] electrode.

6. Supporting electrochemical data (immobilised catalyst)

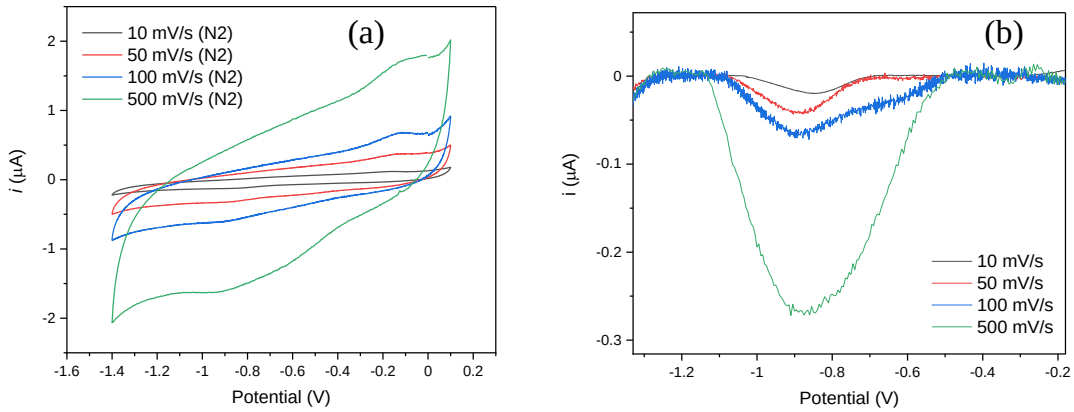

Figure S8. Variable scan rate CVs (a) and with the Ni^{II}/ Ni^{I} reduction peak at -0.90 V shown in detail (baseline corrected) (b) of GCE/[Ni(Cyc)] in 0.1M TBA PF_6 CH_3CN under N_2.

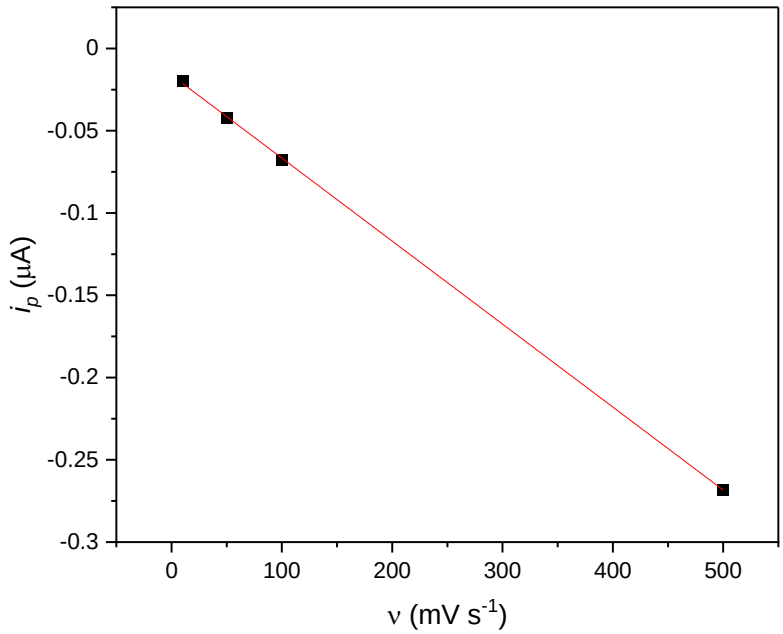

Figure S9. Peak current at -0.9 V from CV vs scan rate of GCE/[Ni(CycPy)] in 0.1M TBA PF_6 CH_3CN under N_2.

$$\Gamma_{theo} = \frac{A}{A_{py} N_A}$$

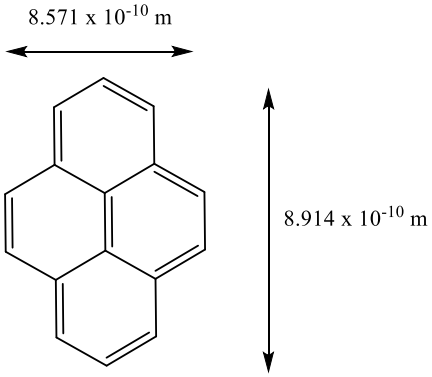

Figure S10 Calculation used to estimate a theoretical surface coverage for a monolayer of [Ni(CycPy)] (Γ_{theo}). Where A is area of the electrode, A_{py} is the area of the pyrene foot print (estimated as shown) and N_A is Avogadro's constant. We assume that the pyrene group lies parallel to the electrode surface and that the closest packing structure can be calculated by approximating the pyrene foot-print to a rectangle. This estimation does not take into account the space required by the C4 linker or the cyclam complex itself. As electrochemical and XPS measurements show that the Ni centre of the cyclam complex is interacting strongly with the

carbon surface we know that our estimated catalyst foot-print is an under estimation, in-line with the measured coverage being ~0.5 that of the estimation.

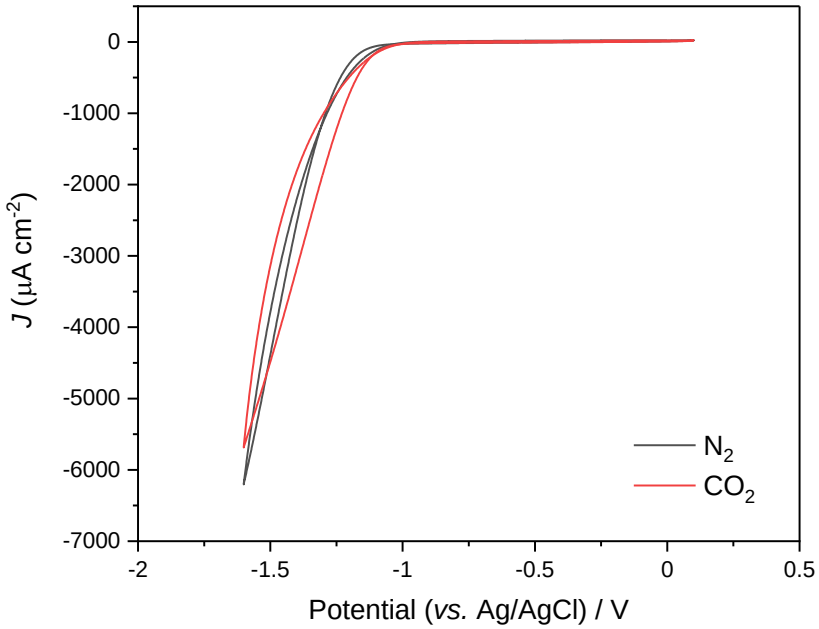

Figure S11. CVs GCE/[Ni(Cyc)] in 0.5 M $KHCO_3$ under N_2 and CO_2.

7. GDE experimental details

A gas diffusion electrode (GDE) was prepared by spray coating down a catalyst ink onto a 10.5 cm^2 area of ELAT LT1400, the back of the GDL had been pre-treated by spraying down 1 mL 5 wt% PTFE solution. The catalyst ink consisted of 10.5 mg of [Ni(cycPy)] electrocatalyst was dissolved in 8 mL methanol, 8 μL Nafion 117 (5 wt%) and 8 μL PTFE (60 wt%). The addition of 10.5mg Ensaco 350G carbon support was also added (figure S13) as part of the GDE optimisation. The catalyst ink was sprayed down onto the GDL, over a hot plate at 50 °C, using a Harder and Steinbeck Evolution air brush at a N_2 pressure of 0.5 bar. The anode was prepared by spray coating a catalyst ink onto a 10.5 cm^2 area on a Ti plate. The catalyst ink consisted of 32 mg RuO_2 dispersed in 1 mL water and 1 mL propan-2-ol and 160 μL of Nafion 117 (5

wt%) sonicated for 30 seconds and was then spray coated down onto the Ti plate, over a hot plate at 100 °C, at a N_2 pressure of 0.5 bar.

GDE electrochemical experiments were conducted in a commercial 4-compartment 10.5 cm^2 GDE flow cell (Electrocell Micro Flow cell). The cell was set-up as a 3-electrode measurement in a gas push through configuration, with gas products sampled from the headspace of the catholyte. The 0.5 M $KHCO_3$ electrolyte solutions were circulated by Verderflex peristaltic pumps, the anolyte and catholyte were circulated at a rate of 22 mL min^{-1} and 12 mL min^{-1}, respectively. The catholyte was pre-saturated with CO_2 for 30 minutes to remove dissolved oxygen. A leak-free Ag/AgCl reference electrode (Alvatek) was inserted close to the surface of the GDE cathode and separated from the RuO/Ti plate anode by a Selemion AMV-N membrane (Bellex). The flow of CO_2 was controlled by a Bürkert Type 8741 mass flow controller and was provided to the cell at a flow of 20 mL min^{-1}. The flow of CO_2 post cell was monitored by a manual bubble flowmeter (Merck). The cell was connected to a BioLogic SP-200 potentiostat. The chronoamperometry measurement was run at -1.4 V vs Ag/AgCl for 2.5 hours.

9. GDE supporting electrochemical data

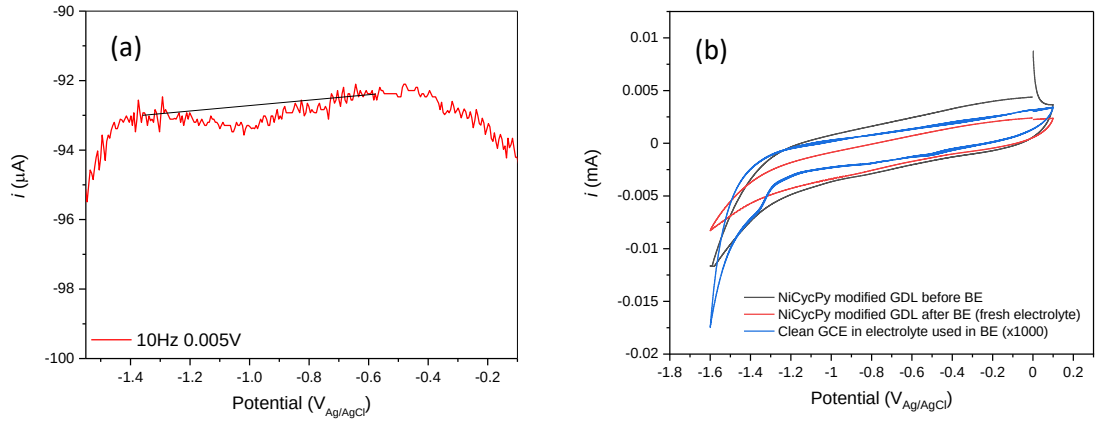

Figure S12 (a) SWV of NiCycPy modified GDE in 0.1M TBA PF_6 CH_3CN under N_2 **(b)** CV comparison of NiCycPy modified GDE in 0.5M $KHCO_3$ (aq) in a standing cell under CO_2 before bulk electrolysis (BE), after BE in fresh electrolyte and a clean GCE (scaled up) in the electrolyte used for BE to show loss of the catalyst from the electrode into the electrolyte.

The peak at -0.95 $V_{Ag/AgCl}$ on Figure S12 (a) has been used to calculate the electrochemically active surface coverage of NiCycPy on modified GDE. We measure the surface coverage to be 1.84×10^{-7} mol cm^{-2} giving us a minimum TON of 13.8 for CO after 15 minutes.

The CVs shown in Figure S12 (b) show the GDE immersed in a conventional electrochemical cell of 0.5 M $KHCO_3$ before and after electrolysis at -1.4 V for 45 minutes. The catalyst is stable in the solution whilst the electrode is at open circuit (solutions are purged for 30 minutes with CO_2 prior to use). However, it is clear that post electrolysis we observe a loss of current suggesting a loss of catalyst from the GDE structure. This is then confirmed by running a clean GCE in the electrolyte used during electrolysis, here we see a peak at -1.36 V indicating the NiCycPy catalyst is in solution. This suggests the loss of selectivity on the GDE over time is due to the pyrene unit being unable to immobilise the catalyst to the carbon support when using a solvent, such as water, where NiCycPy is soluble and when a potential is applied. Although pyrene groups can play an important role in directing the orientation of interaction between an electroactive species and the carbon support, it is clear that in themselves they are not sufficiently stable under reductive conditions to prevent detachment of a soluble catalyst.

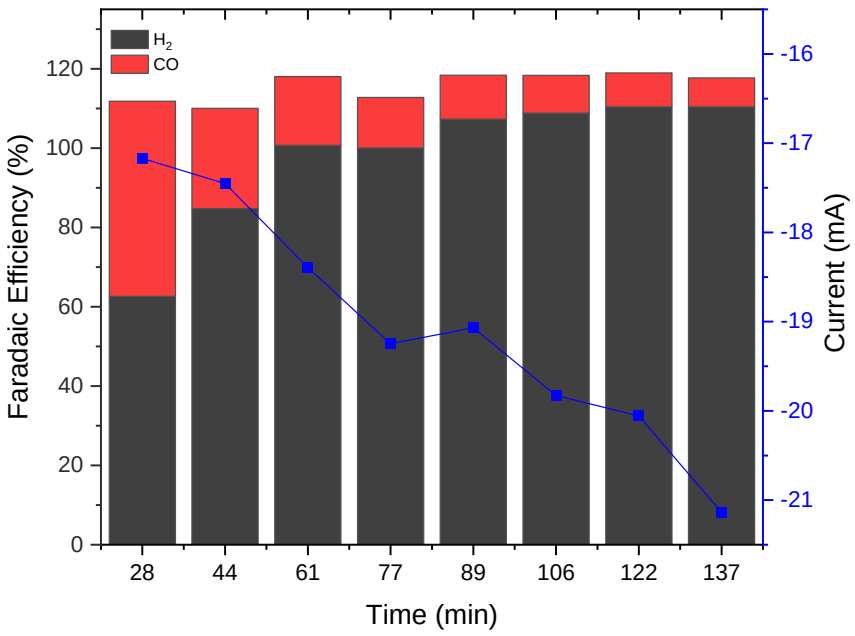

Figure S13 Electrolysis data from a $[Ni(CycPy)]^{2+}$ GDE synthesised with additional Ensaco carbon support with a used in 0.5 M $KHCO_3$ with a CO_2 flow rate of 20 ml min^{-1}.

Fig S13 shows the addition of Enasco 350G carbon support gives higher currents but slightly lower selectivity towards CO. As this does not show a significant improvement, carbon powder was excluded from the GDEs. Future studies will explore additional PTFE treatments to catalyst/carbon powder ink in an attempt to stabilise the enhanced CO_2 reduction activity that is initially observed.

References

1 L. Fabbrizzi, F. Foti, M. Licchelli, P. M. Maccarini, D. Sacchi and M. Zema, *Chem. Eur. J.*, 2002, **8**, 4965–4972.

2 A. Zhanaidarova, C. E. Moore, M. Gembicky and C. P. Kubiak, *Chem. Commun.*, 2018, **54**, 4116–4119.

3 G. Neri, J. J. Walsh, C. Wilson, A. Reynal, J. Y. C. Lim, X. Li, A. J. P. White, N. J. Long, J. R. Durrant and A. J. Cowan, *Phys. Chem. Chem. Phys.*, 2014, **17**, 1562–1566.

4 A. P. Grosvenor, M. C. Biesinger, R. S. C. Smart and N. S. McIntyre, *Surf. Sci.*, 2006, **600**, 1771–1779.

5 Y. J. Leem, K. Cho, K. H. Oh, S. H. Han, K. M. Nam and J. Chang, *Chem. Commun.*, 2017, **53**, 3454–3457.

6 G. Neri, M. Forster, J. J. Walsh, C. M. Robertson, T. J. Whittles, P. Farràs and A. J. Cowan, *Chem. Commun.*, 2016, **52**, 14200–14203.

7 S. P. Roe, J. O. Hill, J. Liesegang, S. P. Roe, J. O. Hill and J. Liesegang, *Transit. Met. Chem. IO*, 1985, 100–106.

8 M. P. Suh, H. R. Moon, E. Y. Lee and S. Y. Jang, *J. Am. Chem. Soc.*, 2006, **128**, 4710–4718.

9 S. Pugliese, N. T. Huan, J. Forte, D. Grammatico, S. Zanna, B. Su, Y. Li and M. Fontecave, *ChemSusChem*, 2020, **13**, 6449–6456.